Catalytic conversion of microcrystalline cellulose to nanocellulose using iron oxide catalysts

Durga Devi Suppiah* & Mohd Rafie Johan

Nanotechnology & Catalysis Research Centre (NANOCAT),

Institute of Postgraduate Studies, University of Malaya, 50603 Kuala Lumpur

Email: durgadevi@um.edu.my

Catalytic conversion of microcrystalline cellulose (MCC) to nanocellulose involves a one-pot homogeneous reaction carried out by the cleavage of β-1,4-glycosidic bonds within the cellulose network. Through this work, the synergistic combination of ultrasonication and catalyst has been proved to be effective in the controlled depolymerisation process of cellulose. Iron oxide being a Lewis acid catalyst has been used to abstract the single electron from the electron-rich C-O bond in cellulose. The iron oxide, maghemite (γ-Fe_2O_3) shows the highest activity as determined by the increase of crystallinity index (CrI%) from 80.62% to 85.63%. The other phases of iron oxide also showed catalytic activity with hematite (Fe_2O_3) at 84.05% and magnetite (Fe_3O_4) at 83.39%. Morphology and particle size analysis clearly show that the nanocellulose have been obtained in the range 78 nm to 220 nm due to the structural dimension measurement of both thickness (diameter) & length. Spectroscopy analysis via Fourier transform infrared and Raman shows no changes to the functional group, hence the chemical composition and integrity of cellulose remains intact. Nanocellulose suspension obtained using maghemite exhibited the highest colloidal stability and surface tension making it more suitable for application.

Keywords: Cellulose, Homogeneous catalysts, Iron Oxides, Lewis acids, Nanocrystalline cellulose

Biomass is a remarkable renewable energy source to compensate the dwindling fossil fuels reserves[1]. Lignocellulose which is one of the materials available in large quantitiy in the world contains 40–50 wt% cellulose[2]. Microcrystalline cellulose (MCC) are partially depolymerized cellulose particles with an average degree of polymerization between 200 and 450[3]. Depolymerization of MCC with cautious control gives cellulose nanocrystals (CNCs), commercially known as nanocellulose. The orientation and alignment of nanocellulose gives rise to diverse characteristics making it a highly potential functional material that can be used in applications such as bio-based reinforcing nanofiller, composite reinforcement, sensors, paper additive and also in tissue engineering and drug delivery[4-6]. In order to make nanocellulose as readily available commercial products, emphasis should be given to large scale production[5]. Typically, in order to achieve nanocellulose with the polymer length around 2–100 nm, commonly used techniques were either chemical (acid hydrolysis or by employing ionic liquid) or enzymatic hydrolysis. However due to the strong hydrogen bonding in the cellulosic structure, low reactivity was achieved by this method[4,7-9]. Heterogenous catalytic depolymerisation using strong acid hydrolysis (e.g., H_2SO_4, HCl, heteropolyacid) combined with mechanical treatment have been used in the recent years for 'deep' depolymerisation of lignocellulosic biomass[7,10,11]. This method applies sonication after acid hydrolysis in order to disband the nanocellulose obtained[12]. Ultra high power sonication increases the dynamic pressure of the cellulose suspension creating gas bubbles that break down immediately after leaving the homogenization gap. This generates shockwaves that disrupts the cellulose walls hence forcing defibrillation[13].

Herein, the highly crystalline nanocellulose has been produced by combining sonication and catalytic hydrolysis of MCC using iron oxide. This study uses iron oxide nanoparticles to catalytically depolymerize MCC to nanocellulose as it is not only non-toxic and cheaper but in addition, the Lewis acid properties act to abstract a single electron from an electron-rich molecule (C-O bond in cellulose) making it the most suitable candidate[1,14,15]. The most effective phase

of iron oxide was identified and the nanocellulose properties were evaluated.

Materials and Methods

Catalytic depolymerization of MCC

Nanocellulose were prepared via sonication technique using a UIP 100hd sonotrode with 12.5 cm frontal area. Then, 5 g of solid MCC sourced from cotton linters (Sigma Aldrich), were loaded into 100 mL water and sonicated at 200 W for 15 min. Thereafter, 0.5 g of three different iron oxide nanoparticles catalyst systems (maghemite, magnetite & hematite) which were synthesised using established methods[16,17] were added and sonicated again at 200 W for 15 min. The colloidal solids were then filtered using gravitational filtration to remove all the water and dried using a vacuum desiccator for 24 h. Since the reaction is homogeneous, the separation and subsequent removal of iron oxide has to be carried out. The 'cake' obtained were added to 300 mL, 0.5 M oxalic acid and stirred for an hour. This step is conducted so as to dissolve all the iron oxide[18]. The product was then filtered and washed till pH 7 was reached to ensure that all the acid has been removed. The white cellulose powder obtained was then dried in a vacuum desiccator for 24 h and subjected to compositional characterization to determine the purity of the cellulose. The process has been illustrated in Supplementary Data, Fig. S1.

Nanocellulose characterization

The obtained nanocellulose was subjected to compositional analysis using Bruker's X-ray Diffractometer (XRD). The XRD diffractograms were obtained using a theta/2theta goniometer and a scintillation counter detector. The data sets were collected in reflection geometry in the range of $2° \leq 2\theta \leq 50°$ with a step size of $\Delta 2\theta = 0.02°$. The degree of crystallinity (CrI) was calculated by subtracting the background using peak high method as shown in eqn 1[19]

$$\text{Crystallinity Index (CrI)} = \frac{(I_{002} - I_{am})}{I_{002}} \qquad \ldots (1)$$

where I_{002} is the peak height at 22° (002) and I_{am} is the height of the amorphous peak of cellulose. This calculation was performed after peak profile fitting. X-Ray fluorescence (XRF) quantitative phase analysis was performed using Bruker's S4 Explorer to determine the composition of Fe before and after nanocellulose purification.

The nanocellulose morphology was analysed using a FEI quanta 200F field emission scanning electron microscope (FESEM). The morphology observation was carried out under low vacuum and an accelerating voltage of 5.0 HV. Intrinsic morphology observation was carried out using Jeoul's transmission electron microscope (TEM). The particle size distribution (PSD) was calculated using Malvern Zetasizer Nano ZS utilizing dynamic light scattering method. The particle size distribution curve was analysed to determine the size of the nanocellulose obtained.

The nanocellulose functionalities were analyzed using Bruker's fourier transform infrared (FTIR) employing potassium bromide (KBr) pellet and Raman spectra, data for which were obtained using a Renishaw inVia Raman microscope with a 50x objective and 785 nm wavelength laser. The laser was set at 5% with 1200 L/mm grating. The surface charge, better known as zeta potential and surface conductivity were analysed using Malvern's Zetasizer Nano. The samples (0.1 g) were sonicated in water for 10 min to disperse prior to measurement. The surface hydrophilicity was measured using a Tensiometer (Dataphysics DCAT 11EC) by employing Wilhelmy plate technique on the freshly prepared nanocellulose suspension.

Results and Discussion

Nanocellulose crystallinity

The obtained cellulosic material after sonication treatment was firstly subjected to XRD analysis to determine the changes in the MCC chemical structure, composition of nanocellulose to iron oxide and also the product crystallinity. The comparitive XRD analysis of MCC is shown in Fig. 1(curve 1). All three diffractograms exhibit similar pattern of the typical crystal lattice of cellulose type 1 matching ICDD PDF File 050-2241. The amorphous region at 19.22° has clearly reduced and this is further confirmed by the crystallinity index calculation using peak high method by subtracting the background[19]. The XRF composition analysis shows that the nanocellulose still contain a very small amount of iron oxide which is also indicated by the brown colour appearance of the nanocellulose obtained (Supplementary Data, Fig. S1). This indicates that the iron oxide nanoparticles had embedded in between the fibrils of the nanocellulose porous structure polymer matrix which were created by the catalytic depolymerisation[20]. The MCC was subjected to

sonication without catalyst and the CrI (%) was calculated to be 80.62. As shown in Table 1, the cellulose crystallinity increased after catalytic sonication treatment. Catalytic treatment using maghemite nanoparticles removes the most amorphous region, increasing the crystallinity to more than 85% while magnetite catalyst though effective, was the weaker catalyst among all three iron oxide systems.

Nanocellulose crystallite sizes were calculated using Scherrer equation. The nanocellulose obtained using hematite has the smallest crystallite size followed by the nanocellulose obtained using magnetite and maghemite catalyst, though the size differences were almost negligible. This shows that by increasing the nanocellulose crystallinity, the amorphous region reduces, thereby impacting the crystallite surface causing the crystallite size to decrease[21].

Catalytic reactions normally take place on material surface. The partial Fe vacancy disorder of maghemite (γ-Fe_2O_3) cubic structure makes it easily activated as catalyst[22]. Similarly, magnetite vacancy disorder also makes it an active catalyst, however the ferromagnetic properties interfere with the catalytic activities. Hematite is the most stable iron oxide phase with no lattice oxygen vacancy, hence it is harder to activate the catalytic properties.

The purification process was successfully carried out (Supplementary Data, Fig. S1) since a white translucent powder of nanocellulose was obtained. The powder was subjected to XRD and XRF analyses to determine the purity level of the nanocellulose as shown in Fig. 2 and Table 1. The XRD obtained for all three samples show the distinctive peaks of nanocellulose at 22° (220) and 14.5° (101). Further confirmation of all samples with XRF shows that more than 90% of Fe was removed. The purification process of nanocellulose using oxalic acid which is a mild acid could also play a role in the depolymerisation of MCC though not very significant, as the acid treatment was not harsh and not accompanied by any physical treatment[23].

Spectroscopic analysis

FTIR spectra (Fig. 3) are almost identical suggesting that the functional groups remained intact after depolymerisation. Internal –OH group of the polymeric cellulose chain remains intact with the IR band at 3430 cm⁻¹ and 2890 cm⁻¹ attributed to –OH and –CH stretching vibration. The IR peak at 1650 cm⁻¹ corresponds to the OH bending of absorbed water. The 1380 cm⁻¹ bending vibration correspond to C-H and C-O groups of aromatic ring in polysaccharides[24] and 1050 cm⁻¹ and 590 cm⁻¹ to C-O-C glycosidic bond[25].

Similarly Raman spectra obtained for nanocellulose, catalysed by different phases of iron oxide are given
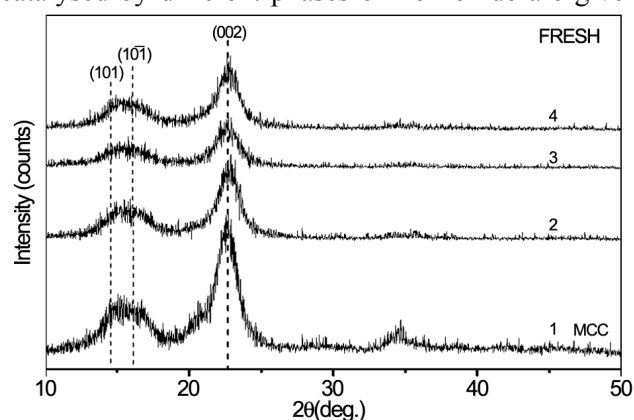

Fig. 1 — X-Ray diffraction pattern of MCC and nanocellulose obtained catalysed by MCC (1), maghemite (2), magnetite (3) and hematite (4).
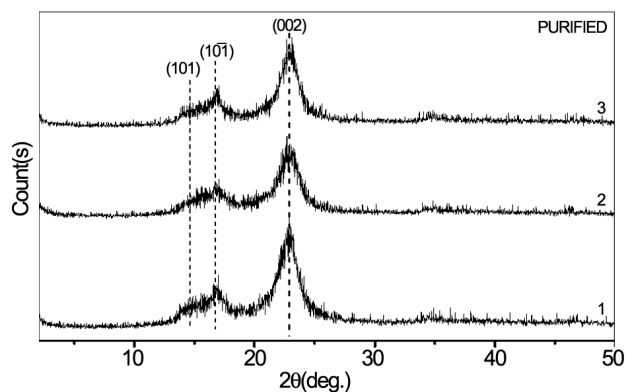

Fig. 2 — X-Ray diffraction pattern of purified nanocellulose obtained, catalysed by maghemite (1), magnetite (2) and hematite (3).

Table 1 — Compositional analysis of nanocellulose obtained after catalytic depolymerization

Iron oxide catalyst	XRF composition (%) before purification			XRF composition (%) after purification			CrI (%)	Crystallite size (nm)
	C	O	Fe	C	O	Fe		
Maghemite	27.15	85.63	1.19	27.27	72.63	0.10	85.63	4.2
Magnetite	27.23	83.39	1.21	27.16	72.74	0.10	83.39	4.2
Hematite	27.17	84.05	0.65	27.22	72.71	0.07	84.05	4.1

Fig. 3 — FTIR spectra of nanocellulose obtained: MCC (1) and catalysed by maghemite (2), magnetite (3) and hematite (4).
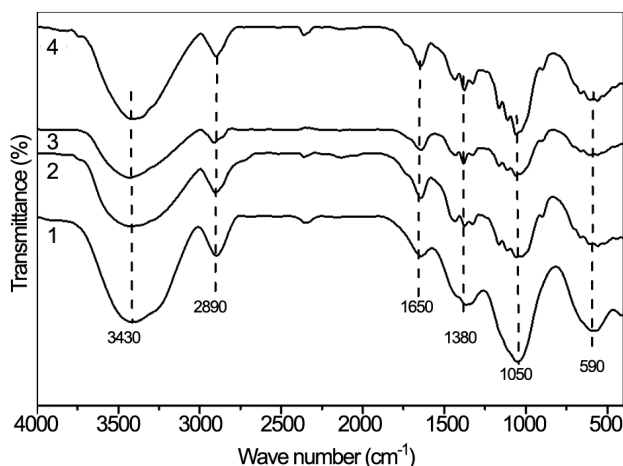

Fig. 4 — Raman spectra of nanocellulose obtained: MCC (1) and catalysed by maghemite (2), magnetite (3) and hematite (4).

in Fig. 4. The catalytic depolymerisation does not affect the chemical structure of cellulose. Peak at 380 cm^{-1} region exhibits the order of crystallinity with NCC obtained using magnetite catalyst which shows the highest crystallinity. Amorphous contributions in the frequency region 250–700 cm^{-1} were not visible suggesting that high crystallinity material was obtained[26].

Surface and colloidal properties

The surface tension of MCC (Supplementary Data, Fig. S2) was clearly influenced by the catalytic depolymerization process. The surface tension of MCC was 53.5 mN/m and significantly increased when sonication aided catalytic depolymerization was applied. Sonication assisted the defibrillation of cellulose fibers hence increasing the concentration of highly polar hydroxide (–OH) and ether group. This creates a stronger hydrophilic-hydrophobic layer thus increasing the surface tension. The Lewis acid nature of iron oxides promotes the breaking of intramolecular hydrogen bonding of the cellulose fibers removing the amorphous region creating good dispersivity[27]. Using magnetite catalyst results in the highest surface tension obtained at 81.91 mN/m due to the ferromagnetic properties[16]. The colloidal stability (Supplementary Data, Fig. S3) increased as shown by higher absolute ZP value than MCC. NCC obtained by use of maghemite catalyst, exhibits highest ZP value, showing that it is the most stable suspension, thus making it the most suitable catalyst for depolymerisation.

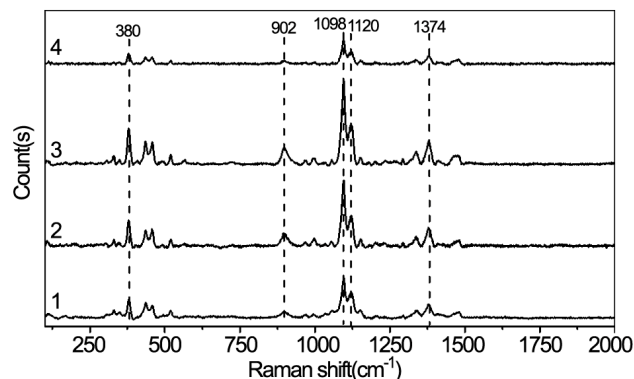The effectiveness of iron oxide as a catalyst for the extraction of electron from C-O bond in cellulose has been proved in the present study. Iron oxide acts as a better Lewis acid as compared to the typical H_2SO_4 treating method besides being less corrosive than sulphuric acid.

Nanocellulose size & morphology analysis

The morphology of nanocellulose obtained after catalytic depolymerisation using solid iron oxide (maghemite) catalyst combined with ultrasonication was scrutinized at the micron and nano level by SEM, TEM and dynamic light scattering analysis (Fig. 3). The untreated commercial MCC in Fig. 5(a) appears to be irregular agglomerated fibrils held together by strong hydrogen bonding between the fibrils[24]. Figure. 5(b) shows that the MCC agglomerate appears to be broken down to smaller aggregates after the ultrasonication assisted catalytic depolymerisation. Further examination conducted by TEM (Fig. 5(c)) shows individual crystalline nanocellulose needles measuring an average of 140 nm in length. These findings were echoed by the particle size distribution (PSD) analysis (Fig. 5(d)) with particles having an average of 140 nm. The average size obtained was similar to the tungstophosphoric acid (PWA) obtained under sonication treatment, though this experiment was conducted under a lower sonication power at 200 W but for a longer period of exposure (15 min)[28]. However, the minimum size obtained was 78 nm while the maximum size obtained was 220 nm. The reason for this variation in size is due to the structural dimension measurement of both the thickness (diameter) and length when observed under similar conditions[29].

Ultrasonication assisted in the delamination of the cellulose polymer by weakening the intermolecular hydrogen bonding thus exposing the amorphous domain of the cellulose chain. This was caused by the ultrasonication acoustic cavities in aqueous solution containing the microcrystalline cellulose. MCC (5 g)
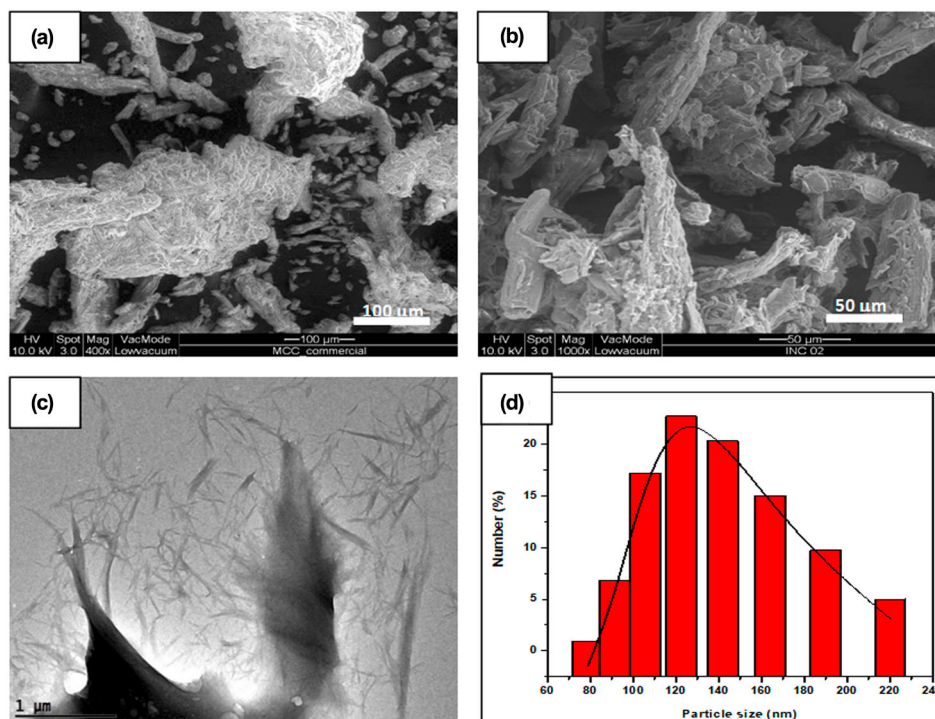
Fig. 5 — (a) SEM image of commercial MCC, (b) SEM image, (c) TEM image, and, (d) Particle Size Distribution (PSD) of nanocellulose obtained using maghemite catalyst.

equivalent to 0.0135 moles was used. The ultrasonication process was carried out for approximately 200 W for 15 min (900 s). Hence a total of 30000 W was used for the cleaving process. Therefore, an average of 222 kJ/mol of energy was required for the cleavage of 1 mole of MCC. The energy by ultrasonication cavitation is approximately 10–100 kJ/mol, which is close to the power needed to break the hydrogen bond, hence disintegrating the amorphous part of the cellulose[13,30]. On the other hand, the existence of maghemite catalyst stimulates the cleavage of glycosidic bonds creating nanocellulose. Upon contact with reaction medium (water), the ionization of maghemite (γ-Fe$_2$O$_3$) results in a valence configuration with Lewis acid nature. This enables the abstraction of single electron from electron-rich C-O bond in cellulose, weakening the intramolecular forces (Fig. 6). With the assistance of ultrasonication, the β-1,4-glycosidic bonds are broken leading to the hydrolysis of amorphous region. Due to the soft nature of the catalyst, delamination of cellulose structure does not take place hence a controlled breaking of bond cellulosic unit takes place and not all the bonds between the cellobiose unit are broken to give single glucose structure.
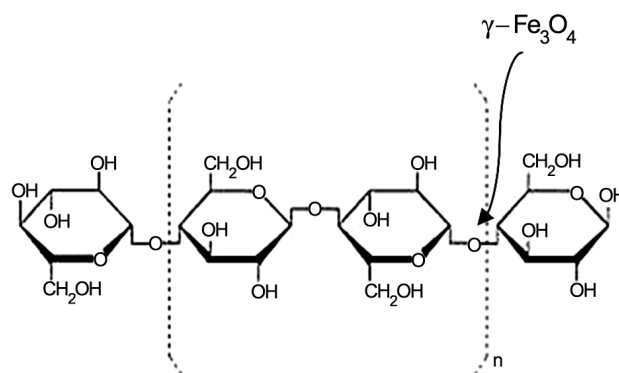

Fig. 6 — Cleaving of β-1,4-glycosidic bonds.

This proves that the nanocellulose can be obtained via catalytic depolymerisation using iron oxide (maghemite) catalysts straying away from the harsh acid treatment[10,24]. The nanocellulose crystals formed were solid gel like structures and disordered as can be seen from Fig. 2(curve 1). The nanoparticles of maghemite catalyst are not water soluble, thus during ultrasonication, as the cavities form, grow and collapse continuously, the solid acid becomes embedded in the nanocellulose framework.

Conclusions

The depolymerisation of microcrystalline cellulose polymer takes place when ultrasonication acoustic cavities expose the amorphous domain of the cellulose chain when ultrasonication weakens the intermolecular hydrogen bonding. The delamination was further aided by the ability of iron oxide to abstract a single electron from the C-O bond of cellulose thus disrupting the hydrogen bond network forcing cellulose defibrillation. The catalytic activity effectiveness was confirmed by the increase of MCC crystallinity to 85.63%. This was further supported by the size and morphology analysis, showing strands of nanocellulose of 140 nm average size. Maghemite was proven to be most active followed by hematite and magnetite. Magnetite was the weakest because of its ferromagnetic behaviour causing it to agglomerate thus inhibiting the active sites that are susceptible to contact with MCC, hence lowering the activity. However, by using iron oxide as a homogenous catalyst, the main problem that was encountered was the separation and recovery of catalyst. This has been resolved by using oxalic acid to dissolve the iron oxide catalysts that were embedded in between the fibrils of the obtained nanocellulose. The effectiveness of homogeneous Lewis acid catalyst such as iron oxide has been proven which may be a new and promising opportunity in the field of catalytic depolymerisation of cellulose in producing nanocellulose.

Supplementary data

Supplementary data associated with this article are available in the electronic form at http://www.niscair.res.in/jinfo/ijca/IJCA_58A(02)265-270_SupplData.pdf.

Acknowledgement

References

1 Azharuddin M, Tsuda H, Wu S & Sasaoka E, *Fuel*, 87 (2008) 451.
2 Collinson S R & Thielemans W, *Coordin Chem Rev*, 254 (2010) 1854.
3 Rebouillat S & Pla F, *J Biomat Nanobiotech*, 04 (2013) 165.
4 Dufresne A, *Mate Today*, 16 (2013) 220.
5 Lin N & Dufresne A, *European Polym J*, 59 (2014) 302.
6 Salas C, Nypelö T, Rodriguez A C, Carrillo C & Rojas O J, *Curr Opini Coll Interf Sci*, 19 (2014) 383.
7 Meine N, Rinaldi R & Schüth F, *ChemSusChem*, 5 (2012) 1449.
8 Foley M, Haverhals L, Klein D, McIlvain W, Reichert M, O'Sullivan D, De Long H & Trulove P, *American J Biom Bioene*, 3 (2014) 68.
9 Bondeson D, Mathew A & Oksman K, *Cellulose*, 13 (2006) 171.
10 Schüth F, Rinaldi R, Meine N, Käldström M, Hilgert J & Rechulski M D K, *Catal Today*, 234 (2014) 24.
11 Tian J, Wang J, Zhao S, Jiang C, Zhang X & Wang X, *Cellulose*, 17 (2010) 587.
12 Filson P B & Dawson-Andoh B E, *Biores Techn*, 100 (2009) 2259.
13 Kalia S, Boufi S, Celli A & Kango S, *Coll Polym Sci*, 292 (2014) 5.
14 Adegoke H I, Adekola F A, Fatok O & Ximba B, *Polish J Env Stu*, 22 (2013) 7.
15 Pouran S R, Abdul Rahman A R & Wan Daud W M A, *J Cleaner Prod*, 64 (2014).
16 Suppiah D D & Abd Hamid S B, *J Magn Magnetic Mater*, 414 (2016) 204.
17 Mohapatra M & Anand S, *Int J Eng, Sci Techn*, 2 (2010) 127.
18 Lee S O, Tran T, Jung B H, Kim S J & Kim M J, *Hydrometallurgy*, 87 (2007) 91.
19 Park S, Baker J O, Himmel M E, Parilla P A & Johnson D K, *Biotechn for Biofuels*, 3 (2010) 10.
20 Khoshkava V & Kamal M R, *Powder Technol*, 261 (2014) 288.
21 Kim U J, Eom S H & Wada M, *Polym Degr Stab*, 95 (2010) 778.
22 Grau-Crespo R, Al-Baitai A Y, Saadoune I & De Leeuw N H, *J Phys: Cond Matter*, 22 (2010) 255401.
23 Kim H Y, Han J A, Kweon D K, Park J D & Lim S T, *Carb Polym*, 93 (2013) 582.
24 Haafiz M K M, Hassan A, Zakaria Z & Inuwa I M, *Carb Poly*, 103 (2014) 119.
25 Tan X Y, Abd Hamid S B & Lai C W, *Biom Bioen*, 81 (2015) 584.
26 Agarwal U P, Reiner R R & Ralph S A, *J Agric Food Chem*, 61 (2013) 103.
27 Miller A F & Donald A M, *Langmuir*, 18 (2002) 10155.
28 Hamid S B A, Zain S K, Das R & Centi G, *Carb Polym*, 138 (2016) 349.
29 Klemm D, Kramer F, Moritz S, Lindström T, Ankerfors M, Gray D & Dorris A, *Angew Chem Int Ed*, 50 (2011) 5438.
30 Tang L, Huang B, Lu Q, Wang S, Ou W, Lin W & Chen X, *Biores Techn*, 127 (2013) 100.